

LOCATING SEISMIC EVENTS IN THE MENENGAI VOLCANIC FIELD OF THE KENYAN RIFT VALLEY

¹E. M. Kamau, ²A. M. Wamalwa, ³F. G. Nderitu

Abstract: Seismic stations comprised of 3 accelerometers, 6 broadband and 5 short period seismometers were installed in Menengai to monitor the level of microseismicity within the volcanic region. This was aimed at identifying the seismic events mapping them and giving an interpretation of their cause. A total of 7241 seismic events with local magnitudes ranging between -1.5 and 2.7 were located and relocated. The results of the relocation show significant epicentral clustering aligned towards the Molo Tectanovolcanic axis, Solai Tectanovolcanic axis and in the caldera. The hypocentral distribution show large depths up to 10 Km in the Menengai caldera and shallower depths of about Km in the northeastern part of the Menengai Volcano. Earthquake swarm activity with rates of more than 150 events per month was noted. Analysis of focal mechanism from 3120 selected earthquakes, show a region predominantly of north east striking faults. The general trend of seismicity indicated by stresses which arise during magma migration in the earth's crust, explains a volcano-tectonic type of earthquake dominating the Menengai Volcanic field.

Keywords: Microseismicity, Earthquake swarms, Focal mechanism, Volcano-tectonic earthquake.

1. INTRODUCTION

Kenya contains the world's most extensive and voluminous alkaline igneous province. Volcanic activity extends 200 km both east and west of the main Rift Valley and is centered on the Kenya "dome" which contains three large volcanoes with calderas (Menengai, Longonot and Suswa) and large volcanic fields at Olkaria and Eburru (Smith, 1994)(figure 1). The central graben rift has been the focus of many geophysical studies. Gravity summaries (Swain, 1992) made to indicate the crustal thickness has been compiled with special attention made on the southern rift (Henry *et al.*, 1990; Swain *et al.*, (1994). Along the Kenya Rift, regional seismic studies of the crust (Henry *et al.*, 1990; Mechie *et al.*, 1994 and Simiyu and Keller, 2001; Simiyu, 2009) showed that there were significant differences in crust structure between the northern, Central and southern parts of the rift valley.

Integrated geophysical analysis carried out by Wamalwa, (2013) in Menengai volcano using resistivity, seismic and gravity data correlated with the surface geology indicate axial gravity high is an intrarift horst block that extends along the axis of most of the rift valley caused by magmatic intrusions into the shallow crust.

Studies on volcanic seismology include monitoring the present status of a volcano, forecasting eruptions, locating magma chambers, and understanding the physical processes that are occurring. Seismic Velocity model along the Rift axis show a 6.1-6.3kms⁻¹ velocity zones lying 5-6km directly beneath the Menengai Volcanic field (Simiyu *et al.* 2001). This is explained in the first major study of the crust of the southern Kenya Rift Valley, the KRISP 90 (Henry *et al.*, 1990). Detailed micro-seismic surveys carried out in Menengai by Simiyu, *et al.* (1997); Simiyu, (2009) and Patlan *et al.*, (2013) show the distribution of events located within the individual volcanic centers. The conjecture about the cause earthquakes in this region is fluid movement and magma migration in the crust. In this study, seismic events were located with hypocenter algorithm and relocated using cross correlation and double difference algorithm to give an insight in to the earthquake activity and stress regime in the volcanic field.

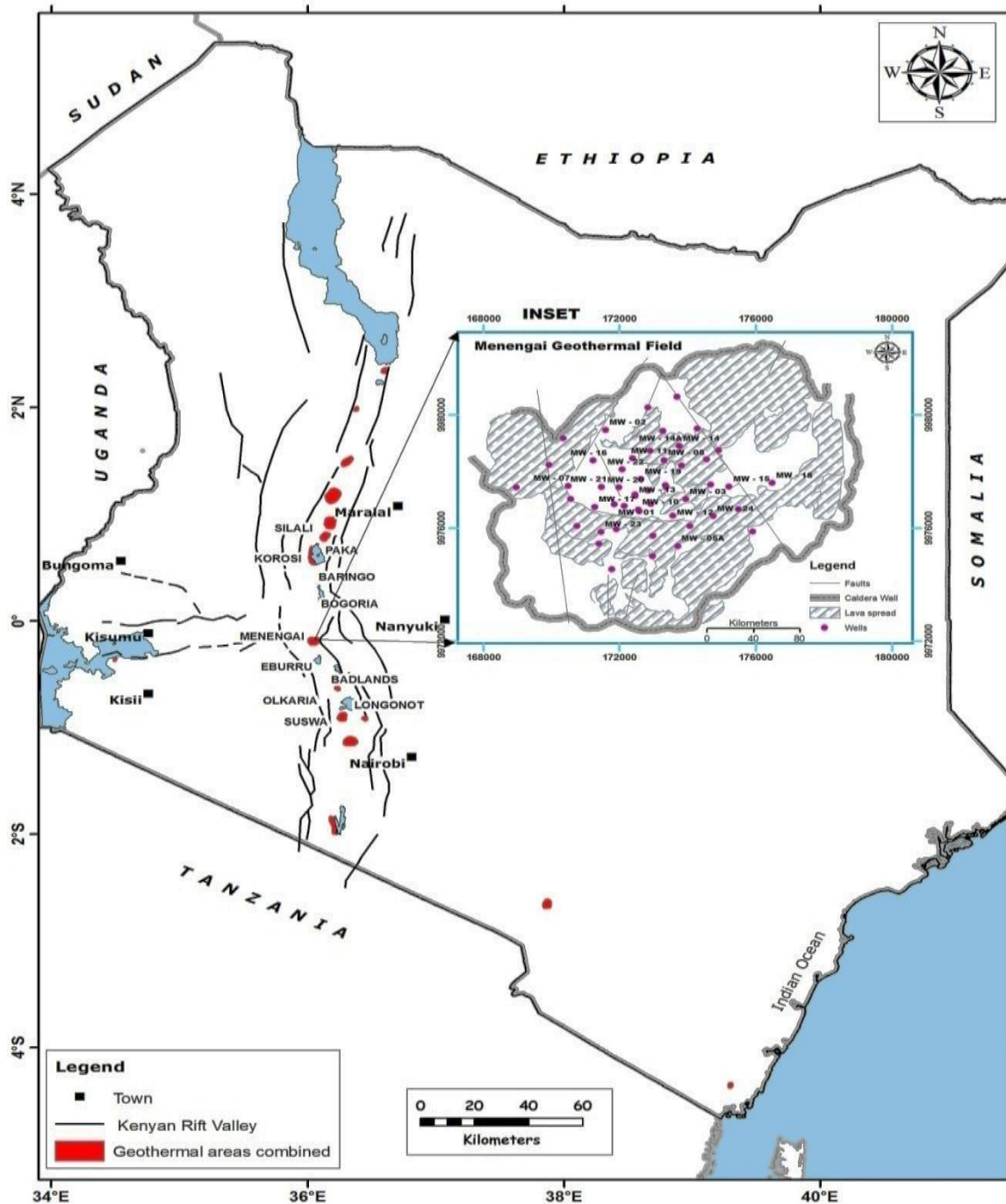


Figure 1: Geographical location of Menengai and other volcanic field and centers in Kenya.

2. GEOLOGICAL SETTING

Menengai volcano, the study area, in figure 2 is a quaternary volcano of predominantly trachytic composition with relatively uniform thickness separated by soil horizons (Leat, 1984) and tuff or pyroclastic intercalations. It is located in the basement of the Mozambique belt, close to the eastern margin of the Tanzanian craton at the intersection of the Nyanzan and the main Kenyan rift. The shield volcano of pre-caldera, syn-caldera and post-caldera formation is characterized by a system of faults and fractures striking in the NNE-SSW direction and the NW-SE direction, which are aligned to the Ol'rongai/Molo Tectonic Volcanic Axis (TVA) and the Solai Tectonic Volcanic Axis respectively (figure 3).

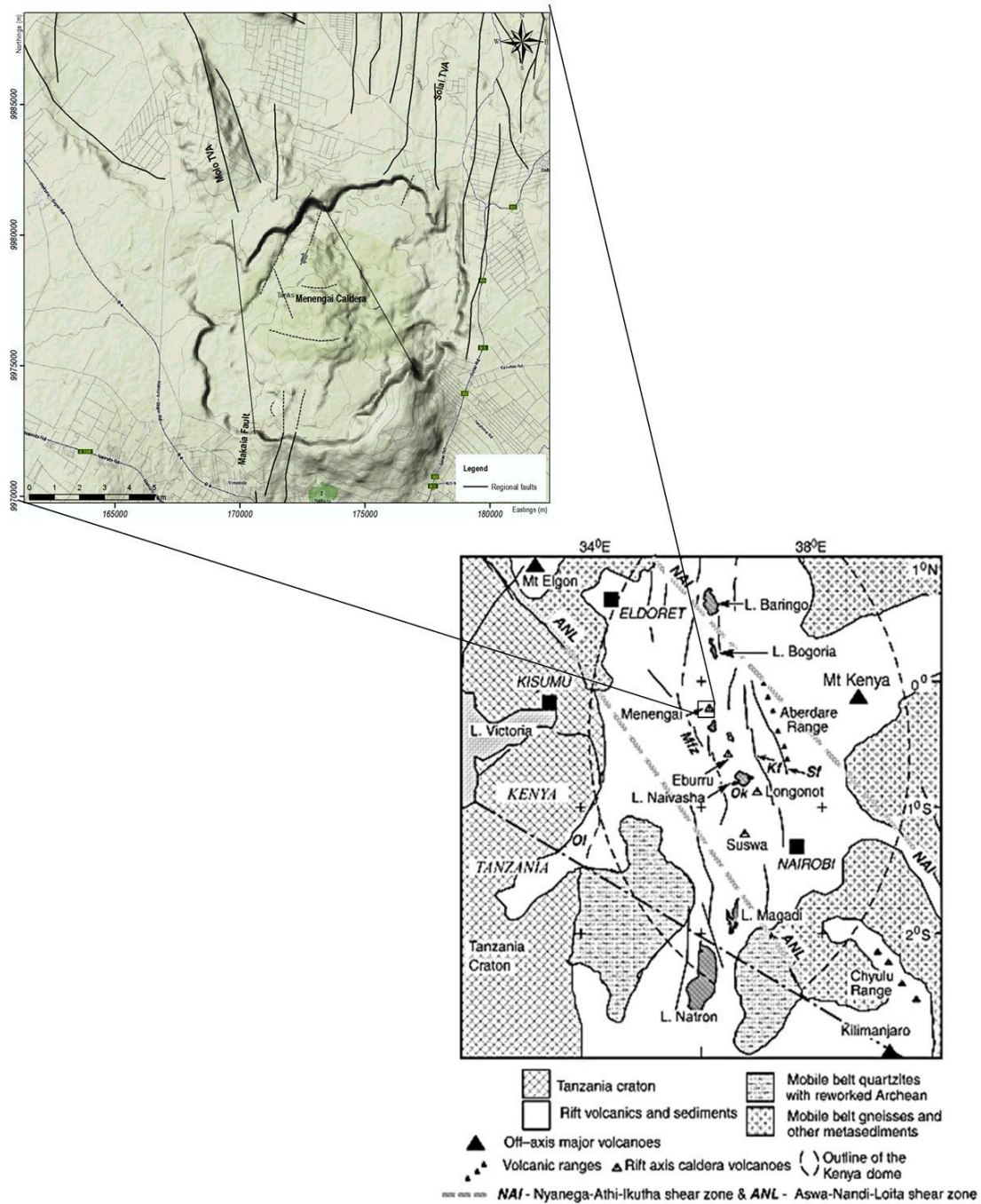


Figure 2: Tectonic setting Menengai volcanic field.

3. THE SEISMIC NETWORK

The seismic network shown in figure 4 were installed in May 2011 and it featured deployment of fourteen broadband Guralp CMG40Ts, CMG3Ts and MINI Seis seismometers around the Menengai study area (table 1). The average distance between stations was approximately between 8 and 15.5 km from the reference centered station MNC1 which is located in the Menengai caldera.

Table 1: Seismic stations locations and the seismometers deployed within the Menengai volcanic field.

Location	Station	Latitude	Longitude	Elevation (m)	Seismometers
Engashura	ANR	36.17344	-0.23659	2022	CMG3T
Bahati	BHT	36.15726	-0.14389	2128	CMG3T
Njoro	BLS	35.96514	-0.33561	2141	CMG40T
Kampi ya Moto	DIGR	35.98462	-0.09644	1714	CMG3T
Kiamunyi	KIMU	36.02485	-0.26634	1945	CMG3T
Lanet	LWS	36.17608	-0.33477	1927	CMG3T
Menengai Crater	MNC1	36.08294	-0.19370	1878	Mini-seis
Menengai West	MNP	35.94658	-0.21791	1999	CMG3T
Ol-Banita	NDG	36.03567	-0.06384	1719	CMG40T
Rigogo	RGO	36.04927	-0.15614	1959	Mini-seis
Solai	SLS	36.12780	-0.09978	1840	CMG40T
Ol-Rongai	TOR1	36.00683	-0.17793	1947	Mini-seis
Menengai View Point	VWP	36.09257	-0.25943	2094	CMG40T
Ol-Kalou	GSS	36.23899	-0.15672	2679	CMG40T

This study was based on data collected from 13 seismic stations (figure 3).

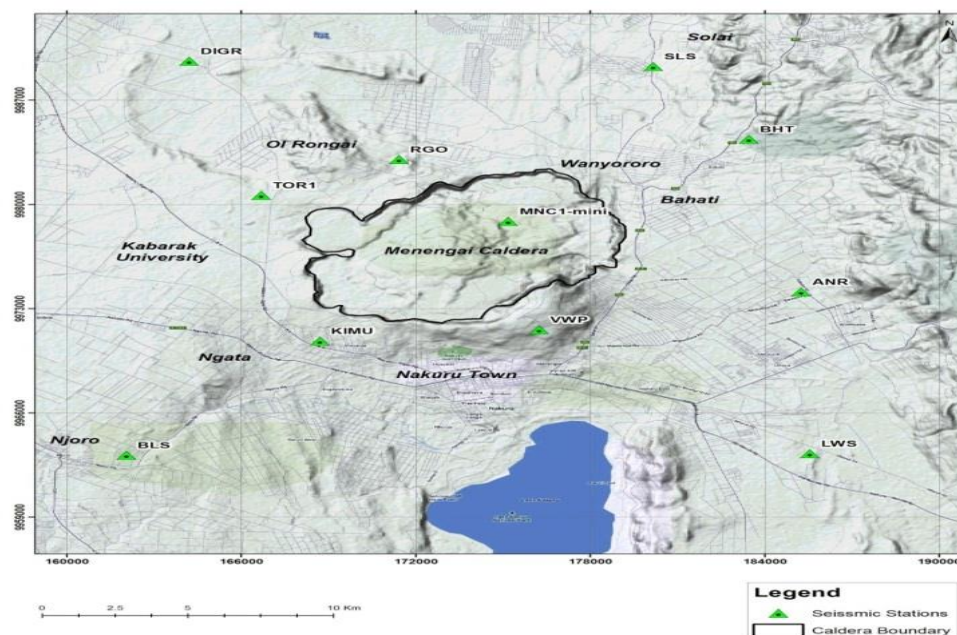


Figure 3: Seismic stations deployed within the Menengai volcanic field.

4. DATA PROCESSING

Reftek waveform data has been analysed in this study to locate seismic events. The acquired digital files recorded are downloaded to the PC. Local events are based on arrival time difference ($T_s - T_p < 3s$) and their hypocenters determined using the Hypocenter earthquake location algorithm (Lienert and Havskov, 1995; Havskov, 2003). Manual picking of the P and S phases of the first-arrival times was carried out on the 115,885 seismograms, of data collected from October 1st, 2011 to October 31st. These included data from local earthquakes with azimuth gaps of $< 180^\circ$ each of which had a minimum of three P and S - phase readings an RMS between 0.00 minimum and 0.03 maximum and a 10^0 back azimuth residual made equivalent to 1 second travel time residual. For earthquake swarm determination, the recorded earthquake swarm activity area is divided into a latitude-longitude grid. Around each grid point, there is a cell with radius smaller. The normalized activity in this study was 1.3626 calculated as the activity in the large cell normalized for area to the small cell, and normalized in time to the window for the swarm.

The local magnitude scale was calculated by determining an amplitude attenuation scale using amplitudes and distances. The Hutton &Boore's (1987) formula used to calculate local magnitude is

$$Ml = a \log_{10}(amp) + b \log_{10}(dist) + c \text{ dist} + d$$

where $a=0.925$, $b=0.91$, $c=0.00087$, $d=+1.31$, \log_{10} is logarithm to the base 10, amp is maximum ground amplitude (zero-peak) in nm and dist is hypocentral distance in km. The constants a, b, c and d are taken from the ESARSWG (Eastern and Southern African Regional Seismological Working Group) (Hollnack and Stangl, 1998; Seht *et al.*, 2001).

The parameters in the local magnitude scale determined as averages of all individual station locations, were computed for every event located by a minimum of three stations. The amplitudes were assumed to be ground displacements (in SEISAN they are ground displacements highpass filtered at 1.25 Hz to resemble Wood Anderson seismograms).

Preliminary seismic events location was done based on Simiyu's, (2009) Menengai and Olbanita Vp-Vs model. The minimum 1-D velocity model was generated through simultaneous inversion of by VELEST program following the Kissling (1998) procedure and the seismic events relocated using waveform cross correlation and double difference algorithm

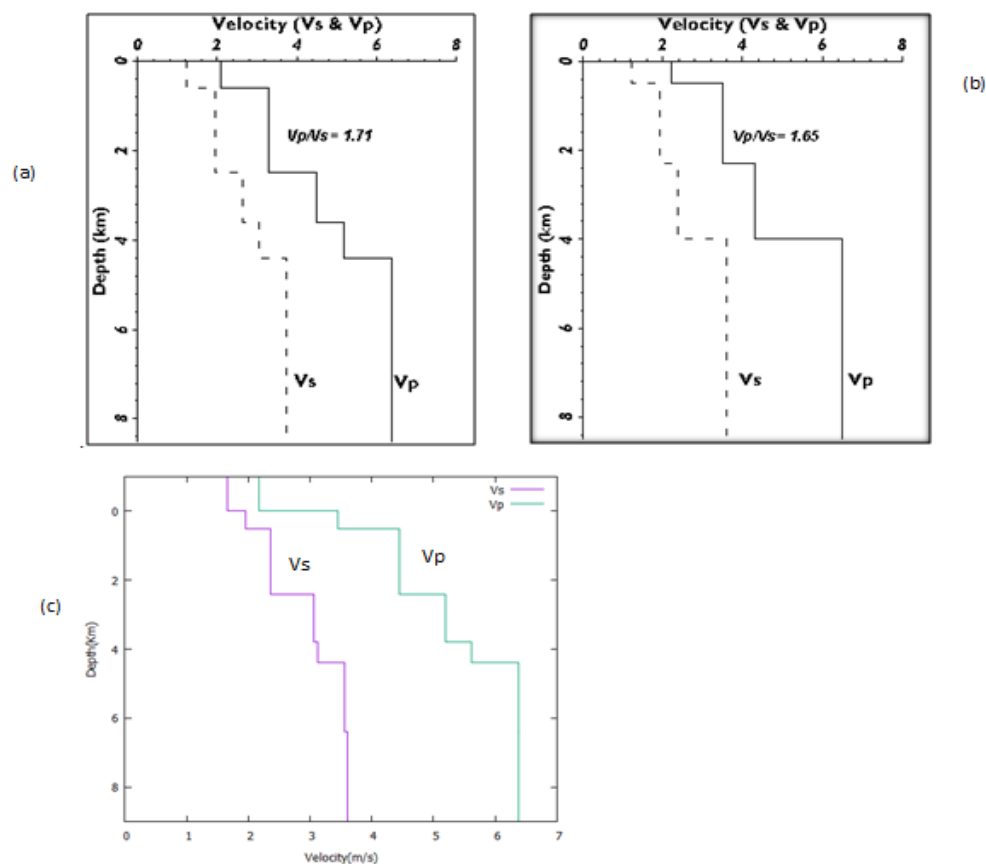


Figure 4: (a) The Olbanita Vp-Vs velocity model (b) Menengai Vp-Vs velocity model by Simiyu(2009) minimum 1-D velocity model generated by the VELEST program used for the relocation of seismic events.

Using the Fortran program FOCMEC fault plane solutions were determined using the double-coupled models of reliable first-motion polarities. Each event was allowed a minimum of three polarities and three amplitude ratios

The earthquake location was based on the least squares inversion and a Gaussian distribution of the arrival time errors. Hypocenter and origin time errors can formally be defined from the residuals of the best fitting hypocenter as;

$$\sigma^2 = \frac{1}{ndf} \sum_{i=1}^n r_i^2$$

with the larger error ellipses corresponding to events outside the network than inside the network

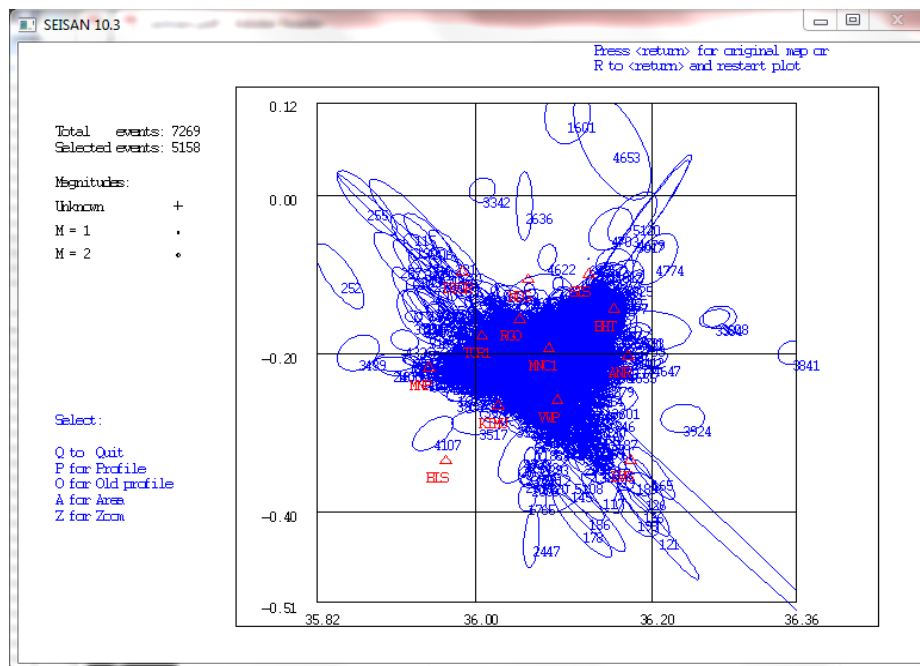


Figure 5: Hypocentral error ellipses.

5. RESULTS

Epical and hypocentral distribution

The results engendered 7269 local earthquakes with 2948 events lying inside the Menengai caldera. 90 earthquake swarms were identified from the dataset with 788 locatable events in the largest swarm and 2 locatable events in the smallest swarm. The local magnitude ranging between -1.5 to 2.1 was obtained for events at depths of 0 to 10 km below sea level which cluster between 2 and 3km below sea level.

The total earthquake swarm activity for 5124 selected seismic events gave a total of 90 swarms without an outstanding event of magnitude greater than one unit from the swarm average. Much earthquake swarm activity was evident during the wet season of the year and less during the dry season of the year (figure 8).

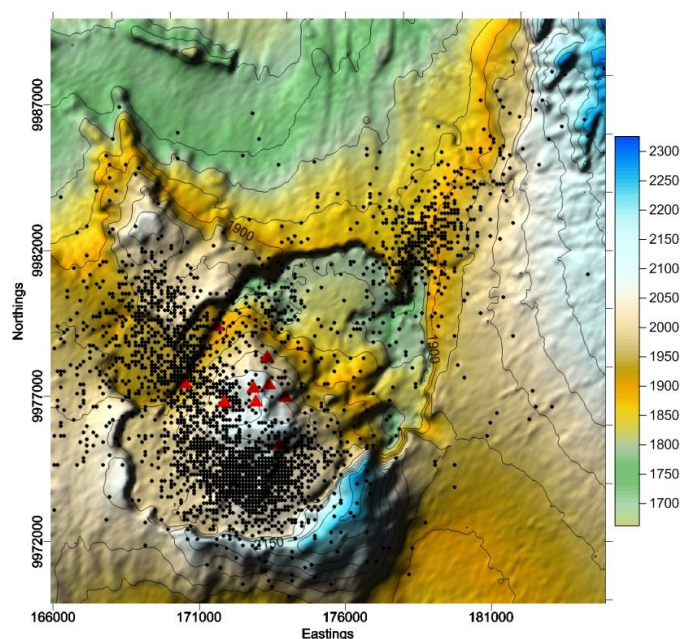


Figure 6: Epical distribution of seismic events on the Menengai Volcanic field.

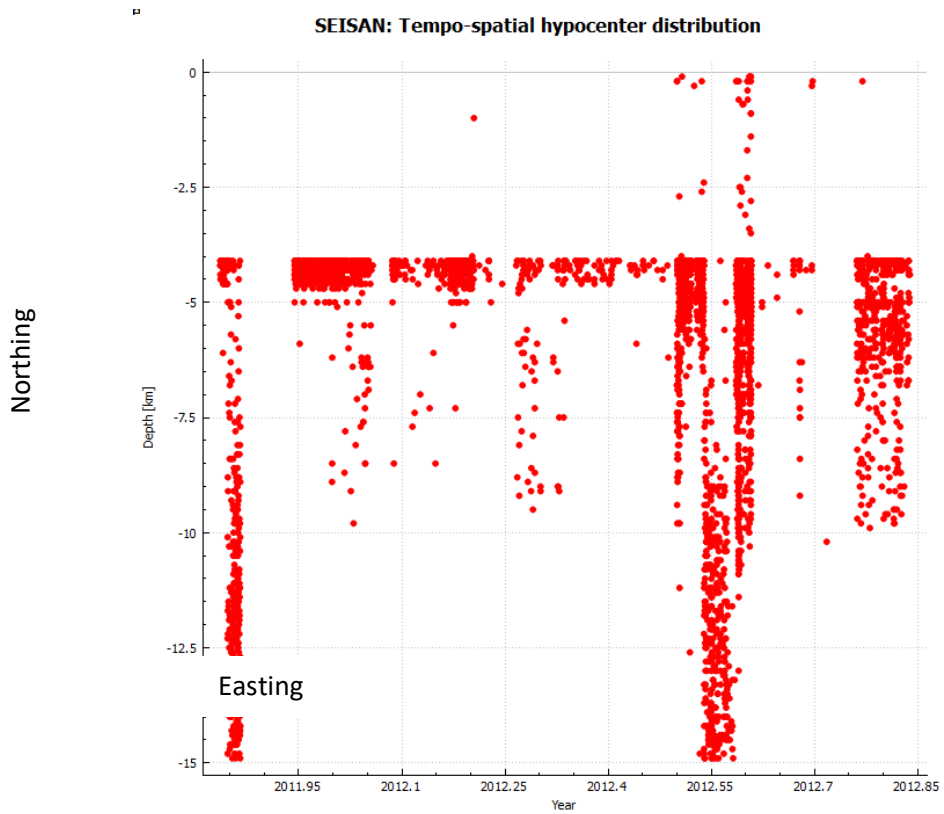


Figure 7: Hypocentral distribution on the Menengai Volcano

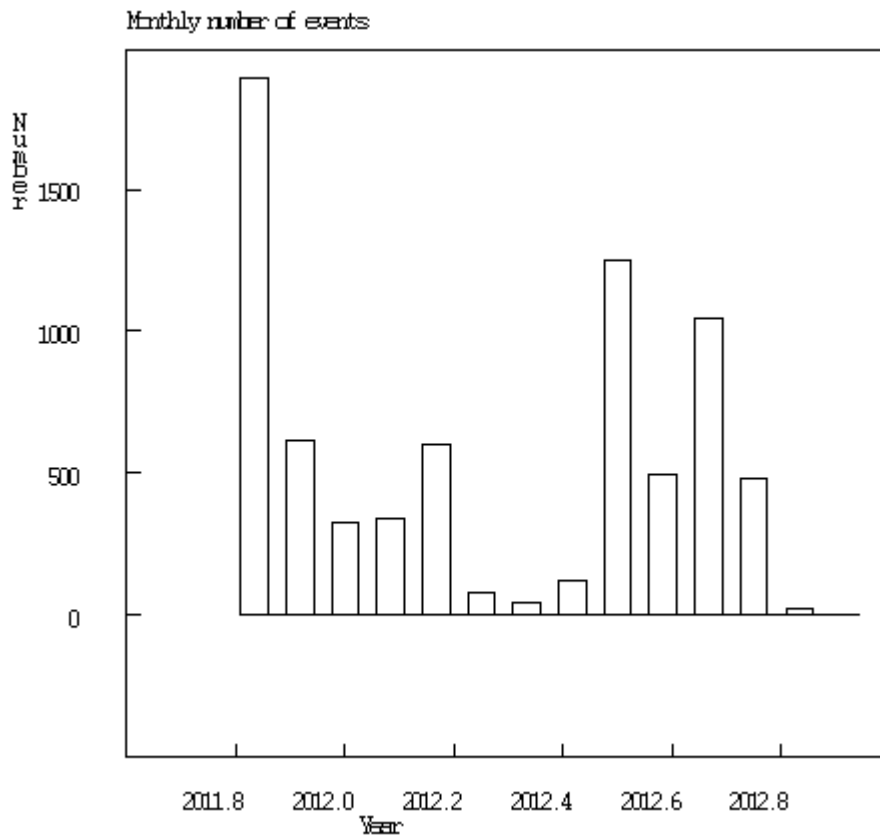


Figure 8: Monthly distribution of seismic events.

Minimum 1-D velocity model

For the minimum 1-D velocity model, 20 iterations were run and 12 best solutions generated for both P and S velocity model, and the two best solution drawn.

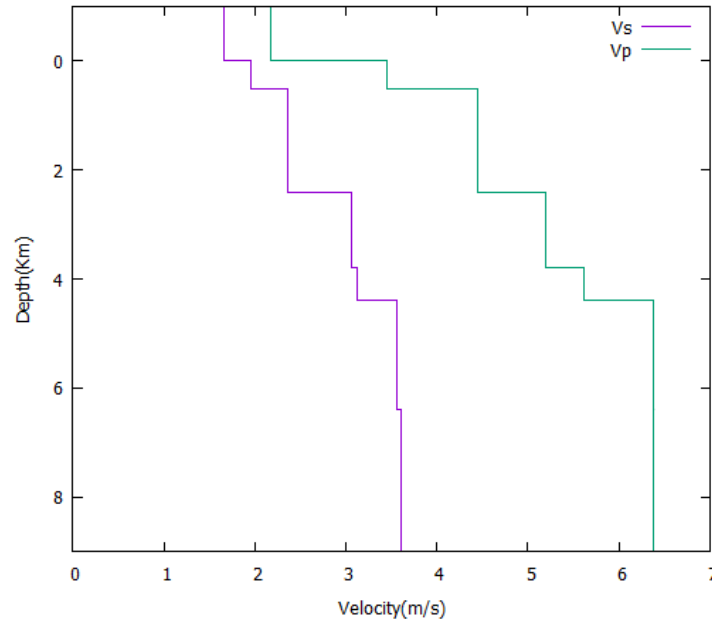


Figure 9: The P and S wave model developed.

Focal mechanism

Focal mechanism was computed for 22 well located events (figure 9) whose magnitudes were sufficient to allow reliable first-motion polarities. Thrust faults with a strike slip component with few normal were noted on the Molo tectano-volcanic axis (9, 10, 11 and 12). Thrust fault with a few oblique reverse faults were noted on the Solai tectano-volcanic axis (1, 2, 4, 5, 6 and 7). At Menengai central strike slip faults, normal and thrust faults with strike-slip components were evident (3,8,13,14,15,16,17,1,19,20,21 and 22).

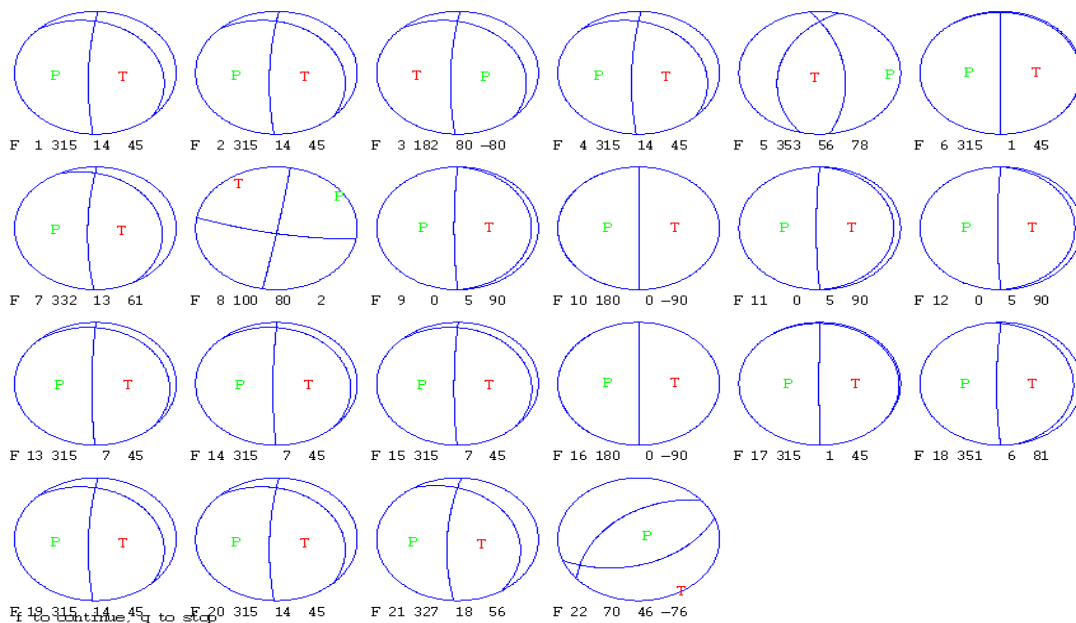
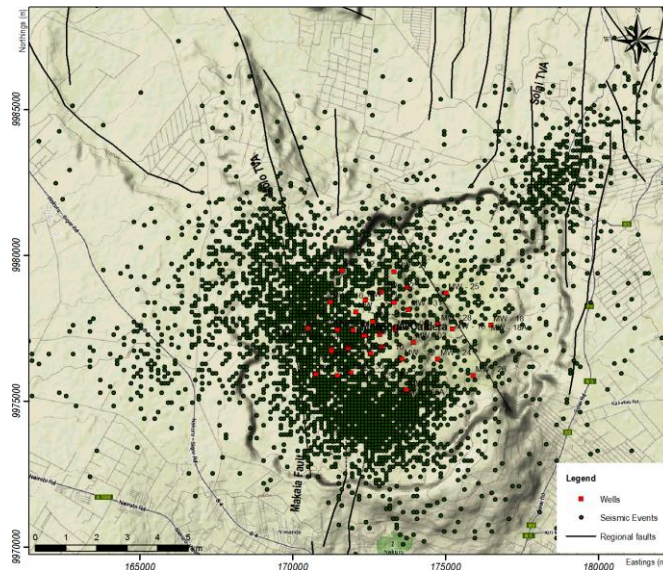


Figure 10 (a): 22 fault pane solution.

6. DISCUSSION OF RESULTS

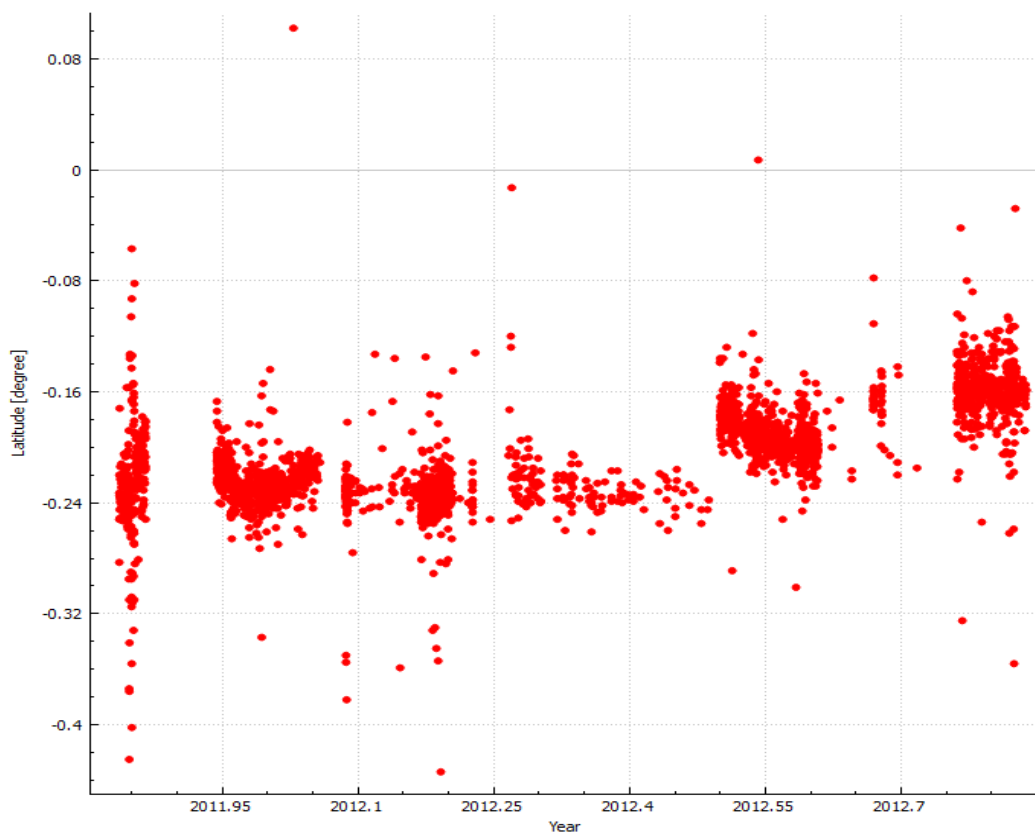
Epicentral and Hypocentral Distribution

The epicentral distribution identified the seismically active regions in the Menengai volcanic field. The clustering of the seismic events is aligned to the Northeast- Southwest direction, central location and the Northwest- Southeast direction along the major fault lines; Molo and Solai tectanovolcanic axes. Local stress conditions may instead favour failure along fault zones of different orientation. There is an inferred NW-SE trending fissure at the centre of the Menengai caldera resulted from transform faulting.



P

SEISAN: Tempo-spatial hypocenter distribution



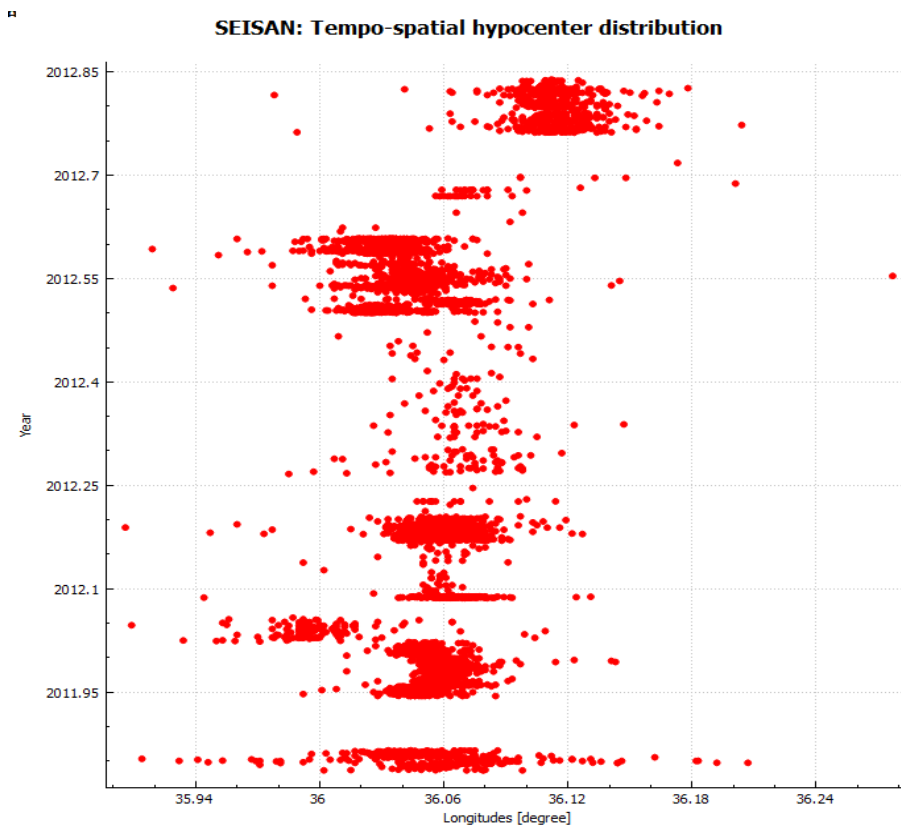
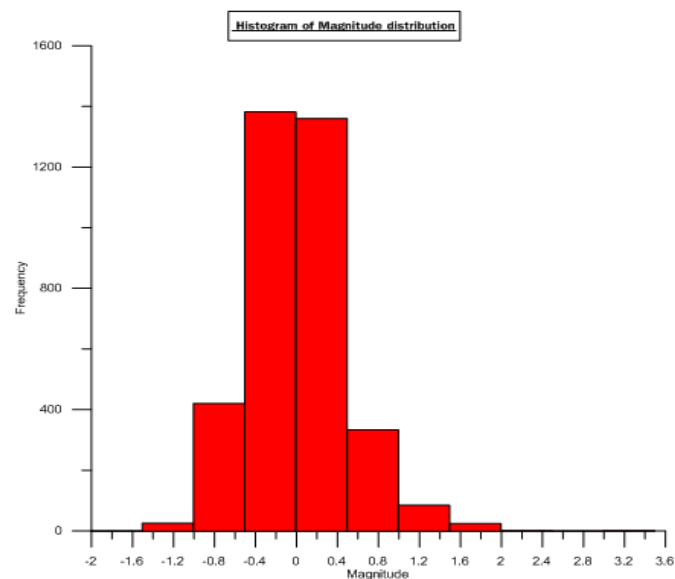


Figure 10 (b): The epicentral and hypocentral distribution of the earthquakes recorded in Menengai volcanic field.

The pattern the events form was a similar to the seismic activity located by Simiyu, 2009 on the Solai and the Ol'rongai region.

A total of 2689 seismic have been located in the Menengai caldera. It is normal for large calderas to show frequent signs of unrest, the vast majority of which are not precursors to eruptions. This adds to the uncertainty in dealing with earthquake swarms at calderas: false alarms are more likely, but large eruptions are also possible. Daily occurrence of the earthquakes with local magnitudes $M_l < 3.0$ is ranging from 0 to 265 events and depths of 0 to about 8.5 Km was noted.



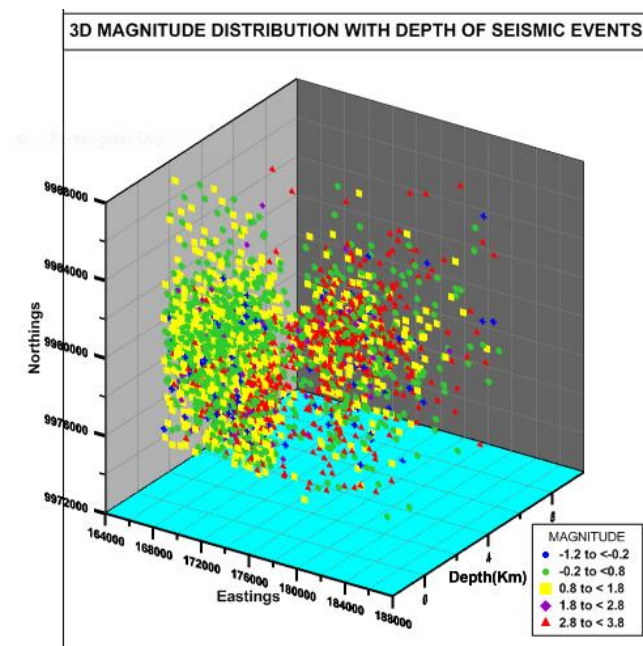


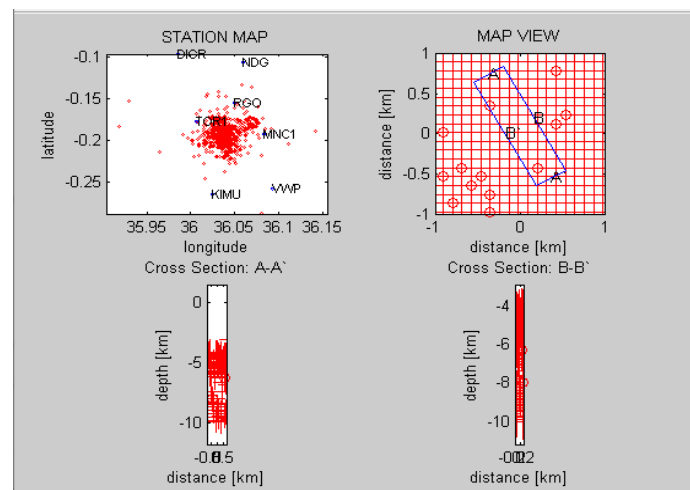
Figure 11: Histogram of magnitude distribution and the 3D magnitude model.

Swarms of microearthquakes (majority of them with magnitudes of about 0) have been recorded on different volcanoes of the world (e.g., Nuñez-Cornu et al., 1994; Orozco-Rojas, 1994; Neuberg et al., 1998; Carniel et al., 2006; Iverson et al., 2006; Macedo et al., 2008; Waite et al., 2008; Varley et al., 2010; Zobin et al., 2010). Comparative to the Menengai volcanic field seismic signals are numerous, low-amplitude, and form families of similar records.

The events were classified as A-type and B-type volcanic events with few micro-tremors evident following a main shock-after-shock and swarm sequences (Zobin, 2013). These are volcano-tectonic earthquakes generated by fluid movement within the earth and stresses, which arise during magma migration in the Earth's crust.

Minimum 1-D velocity model

The 3120 relocated seismic events, using the minimum 1-D velocity model, form one major cluster of 720 events at the caldera aligned towards Molo Tectanovolcanic axis, by applying the least squares regression in the double difference algorithm. Cross-correlation test performed on the initial seismic records of microearthquakes observed between October 2011 and October 2012 shows that the waveforms have a good intercluster correlation. The minimum 1-D velocity gave a better picture of the most seismogenic zones for the events located in Menengai volcanic field (figure 11). The hypocentral depths of the relocated events is constrained to above 10km below sea level.



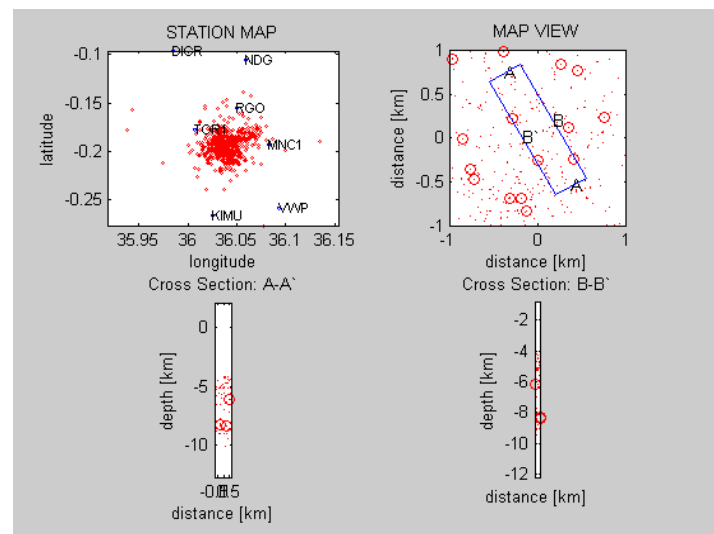


Figure 12: Preliminary 3120 seismic events located in (a) and (b) shows relocated seismic event using the 1-D minimum and double-difference algorithm.

Focal mechanism

More than half of the focal mechanisms imply tensional strain on the faults and fractures within and around the Menengai Volcano, with one of the nodal planes striking NE-SW, and right lateral slip if that plane is chosen as the fault plane. The fault nature of volcano-tectonic earthquakes was thrust/transverse fault, normal fault, oblique reverse and strike-slip. It was constrained by the regional and local tectonic stress systems. There is an inferred NW-SE trending fissure at the centre of the Menengai caldera resulted from transform faulting. The focal mechanisms at the center of the Menengai caldera related to fissure eruptions, revealed the coincidence of its one fault plane with the strike of the eruptive fissure.

Seismicity in the region was caused by shear failure as the result of slip on joints. This occurs when the effective stress is reduced by increasing the pore fluid pressure. Small eruptions and many phreatic (water driven) eruptions, in contrast, involve much smaller amounts of magma, and have subtle precursors or sometimes no precursors.

7. CONCLUSION

The seismic events in Menengai volcanic field are considered volcano-tectonic earthquakes generated by stresses caused by the shear fracturing during magma movement from depth to the Earth's surface through conduits and dykes. This level of seismicity reflects the level of volcanic activity, and suggests that there is a constant long-term probability of eruption, usually assumed to be a Poisson process. This means that eruptions behave as a random variable, and have no memory (mathematically) of previous eruptions. The average rate of eruptions is also assumed to be constant, and the probability increases when earthquake swarms occur. The main physical processes monitored, however, are those associated with magma intrusion. Thus, there will always be a false alarm rate because some intrusions remain at depth whereas others reach the surface and erupt.

The minimum 1-D velocity model ensures accurate earthquake location. It allows one to make some inference on the deep structures revealed in the lower crust. Hypocentral depths of the earthquake appear to be better constrained.

Spatial orientation of the seismicity was coplanar with the fissure at the centre of the caldera and the regional faults, suggesting a pre-existing fracture zone was being re-opened and expanded. Shear failure allowed existing fractures to open in the direction of the maximum principal horizontal stress. The knowledge of temporal variations of the spectral source parameters may allow the description of the main events during the eruptive process.

Absence of earthquake magnitudes larger than 3, indicate a region of low stress regime, fluid circulation and hydrothermal alteration, hence low risk to the surrounding community. This gives a good reason for a continuous seismic network operation, to monitor the volcanic system and for public safety.

REFERENCES

- [1] Henry, W.J., Mechie, J., Maguire, P.K.H., Khan, M.A., Prodehl, C., Keller, G.R., Patel, J.P., (1990). A seismic investigation of the Kenya Rift valley. *Geophys J. Int.* 100, 107–130.
- [2] Kissling, E., Ellsworth, W. L., Eberhart-Phillips, D., and Kradolfer, U. (1994). Initial reference model in local earthquake tomography. *J. Geophys. Res.*, 99:19635{19646.
- [3] Lienert, B. R. and Havskov J.,(1995). A computer program for locating earthquakes both locally and globally. *Seism. Res. Lett.* 66, 26–36.
- [4] Ottemöller, Voss and Havskov, (2014). *Seisan earthquake analysis software for Windows, Solaris, Linux and Macosx. Version 10.3*
- [5] Patlan E., Wamalwa A., Kaip G., Grijalva A., and Velasco A.A. (2013). Microseismic Study of Menengai Caldera: Geothermal Prospect in the Central Kenya Dome
- [6] Simiyu, S.M., Keller, R.G., (1997). Seismic and gravity inter-pretation of the shallow crustal structure in the Southern Kenya Rift Valley., *Geophys J. Int*
- [7] Simiyu S. M and Keller G. R., (2001) An integrated geophysical analysis of the upper crust of the southern Kenya rift., *Geophys. J. Int* 147, 543–561
- [8] Simiyu, S.M., (2009). Application of micro-seismic methods to geothermal exploration: examples from the Kenya rift, *United Nations University and LaGeo*, 11-27.
- [9] Smith M., (1994). Stratigraphic and structural constraints on mechanisms of active rifting in the Gregory rift, Kenya, in *Crustal and Upper Mantle Structure of the Kenya Rift*, eds Prodehl, C., Keller, G.R. & Khan, M.A., *Tectonophysics*, 236, 3–22.
- [10] Swain, C.J., (1992). The Kenya rift axial gravity high: a re-interpretation, *Tectonophysics*, 204, 59–70
- [11] Swain, C.J., Maguire, P.K.H., Khan, M.A., (1994). *Geophysical experiments and models of the Kenya Rift before 1989. In: Keller C., Khan G.R., M.A. _Eds., Crustal and Upper Mantle Structure of the Kenya Rift. Prodehl, Tectonophysics 236 23–32.*
- [12] Wamalwa A.M., Mickus K. and Serpa L.,(2013) Geophysical characterization of the Menengai volcano, Central Kenya Rift from the magnetotelluric and gravity data. *Geophysics (2013) 78 (4): B187-B199.*<https://doi.org/10.1190/geo2011-0419.1>
- [13] Zobin V (2013). *Introduction to volcanic seismology: Vol. 6 (Developments in volcanology)*, Elsevier Science, Amsterdam